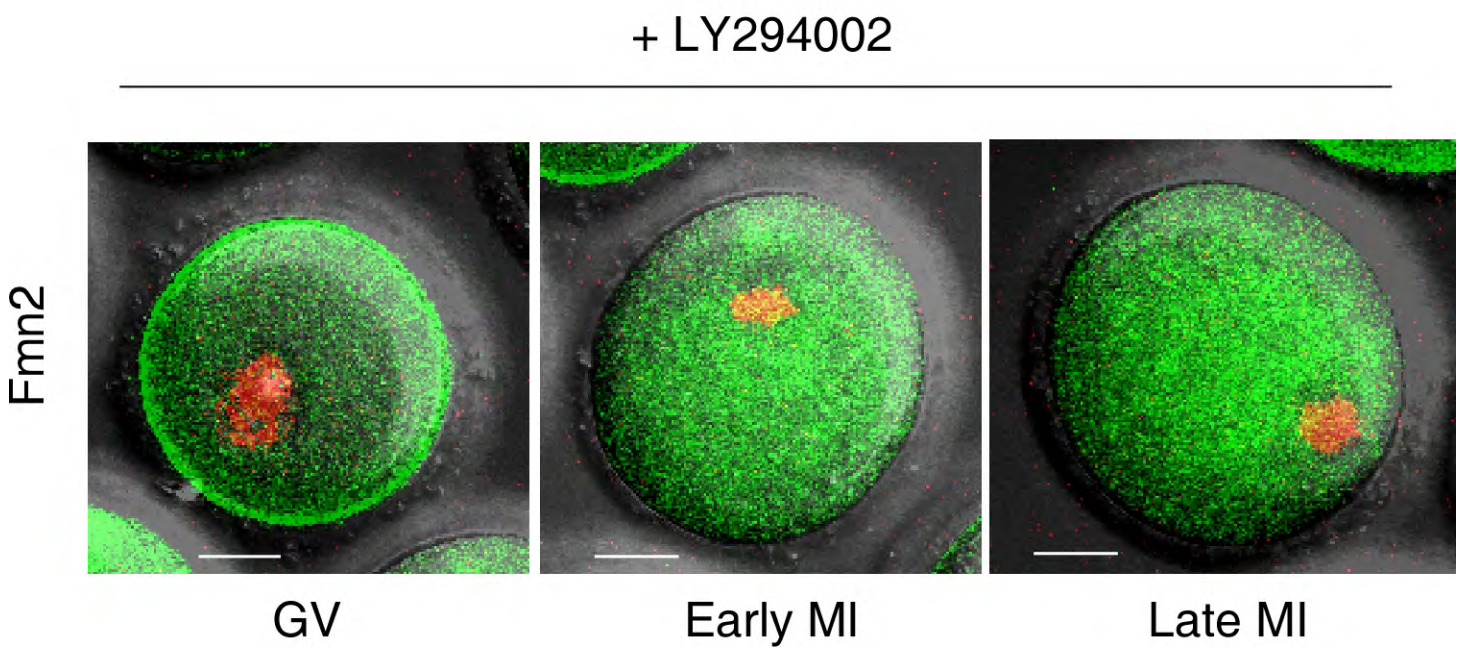

Fig. S1. Diffusion of EGFP-Fmn2 in cytoplasm of oocytes treated with LY294002 (20 μM). DNA (red) was labeled by Hoechst 33258. Images were obtained by confocal microscopy at different stages of meiosis I. GV, germinal vesicle stage; MI, metaphase I. Scale bars, 20 μm.

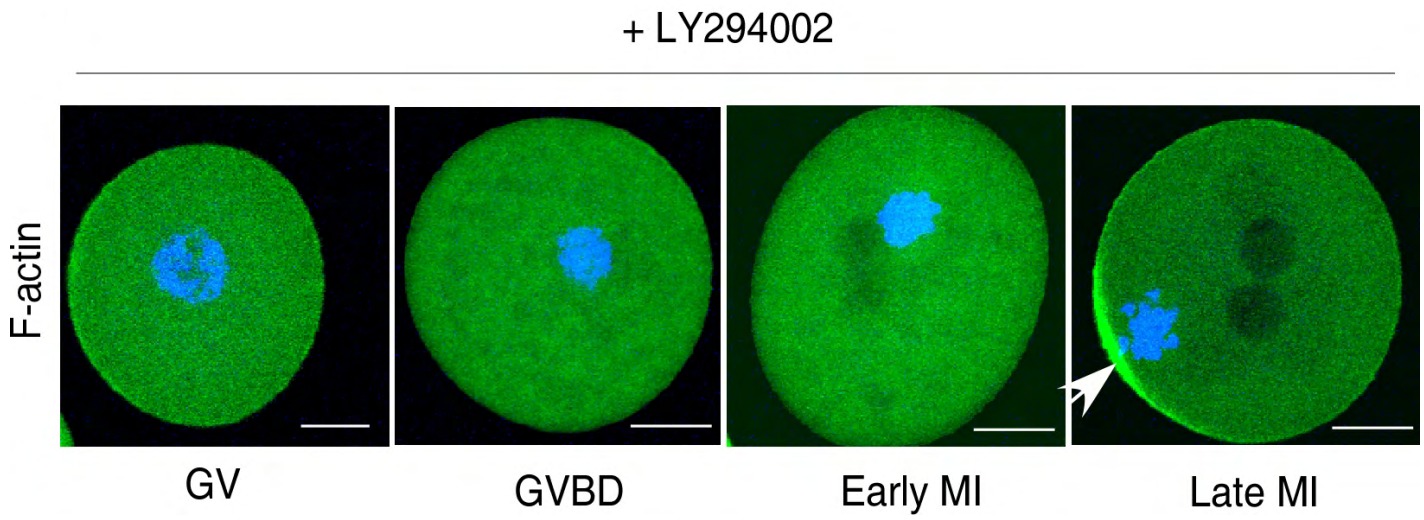

Fig. S2. Diffusion of F-actin in cytoplasm of oocytes treated with LY294002 (20 μM). DNA (blue) was labeled by Hoechst 33258 and actin was detected with EGFP-LifeAct. Images were obtained by confocal microscopy at different stages of meiosis I. LY294002 treatment did not affect the cortical F-actin cap (arrow). GV, germinal vesicle; GVBD, germinal vesicle breakdown; MI, metaphase I. Scale bars, 20 μm.

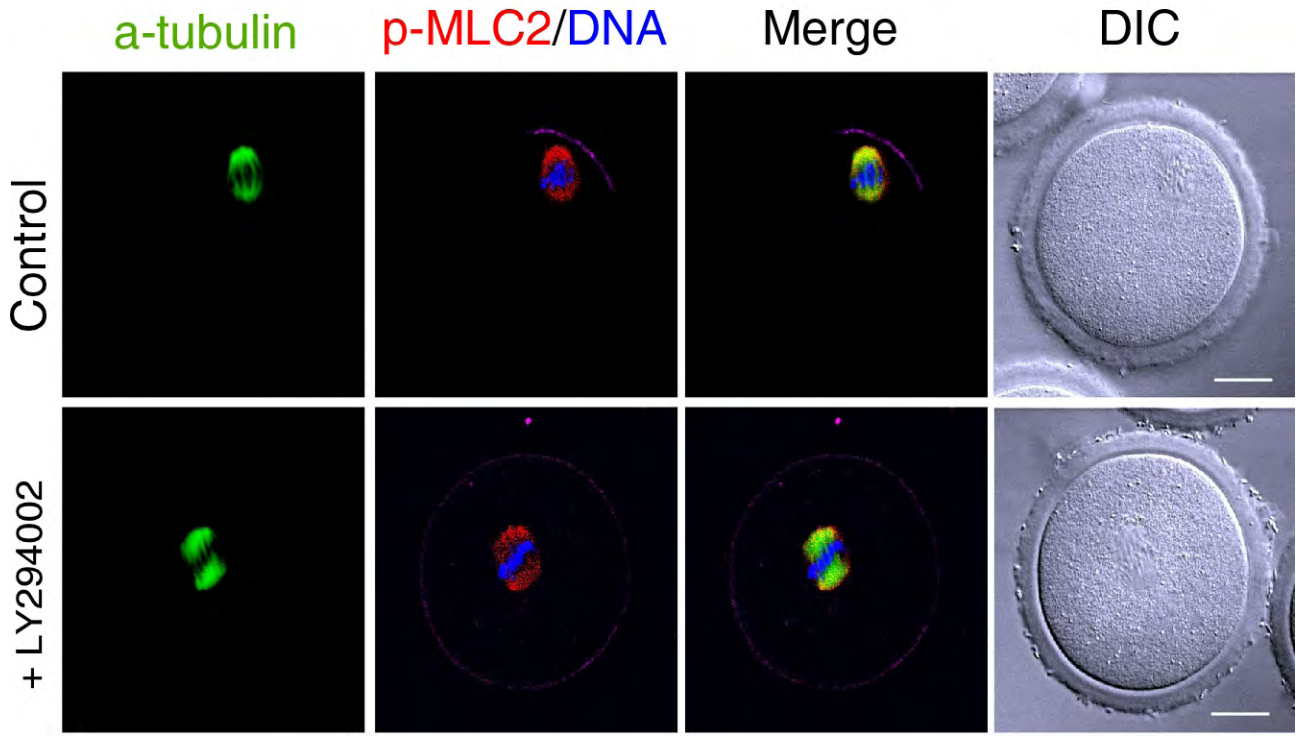

Fig. S3. LY294002 treatment did not influence the phosphorylation and localization of myosin 2. Immunofluorescent staining of the phosphorylated light chain of myosin 2 (p-MLC2) in oocytes treated with LY294002 (20 μM) or vehicle alone (lower and upper panels, respectively). Spindles were counterstained with antibody against α-tubulin. Cortical F-actin was visualized by phalloidins (pink). Scale bars, 20 μm.

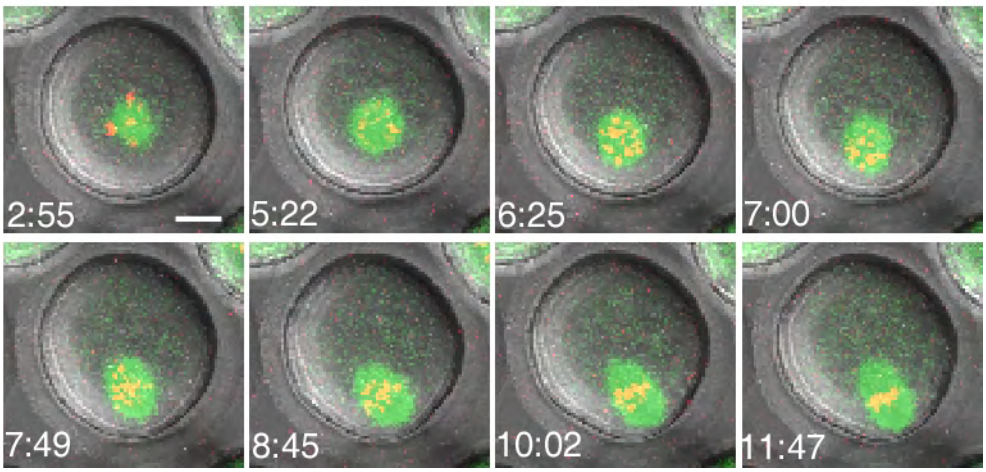

Fig. S4. Spindle movement in oocytes from wild-type littermates of *Mater*$^{-/-}$ mice (C57BL6×SV129). Spindles were visualized with EB1-GFP and DNA (red) was labeled by Hoechst 33258. Images were taken from time-lapse confocal microscopy at indicated scan time points (hr:min). Scale bars, 20 μm.

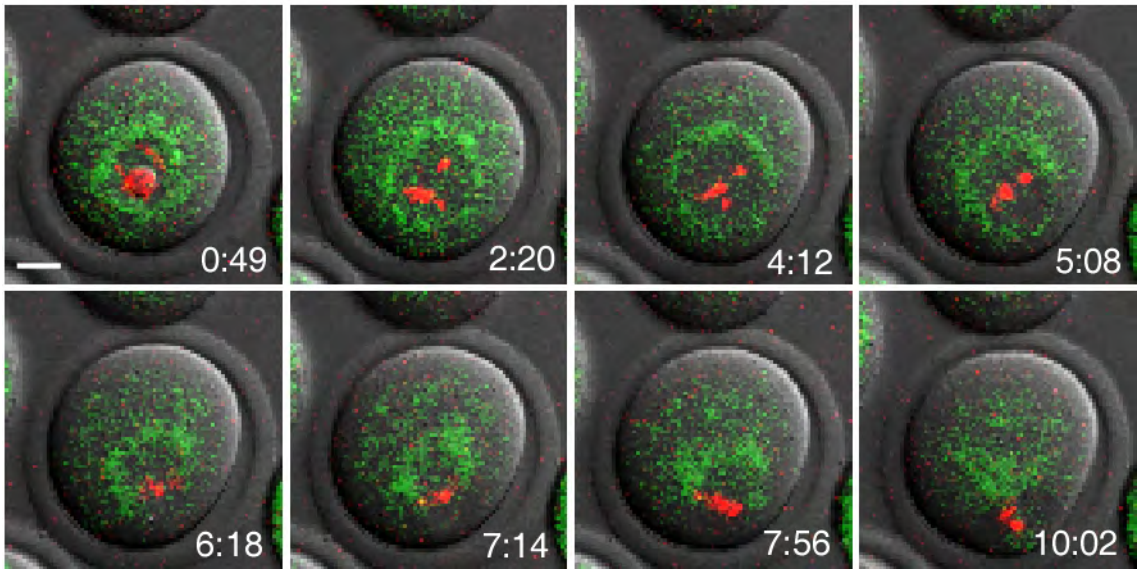

Fig. S5. Synthesis of PtdIns(3,4,5)P_3 during meiotic maturation of oocytes from wild-type littermates of *Mater*$^{-/-}$ mice. PtdIns(3,4,5)P_3 was monitored by PH-Akt-GFP. DNA (red) was labeled by Hoechst 33258. Images were taken from time-lapse confocal microscopy at indicated scan time (hr:min). Scale bars, 20 μm.

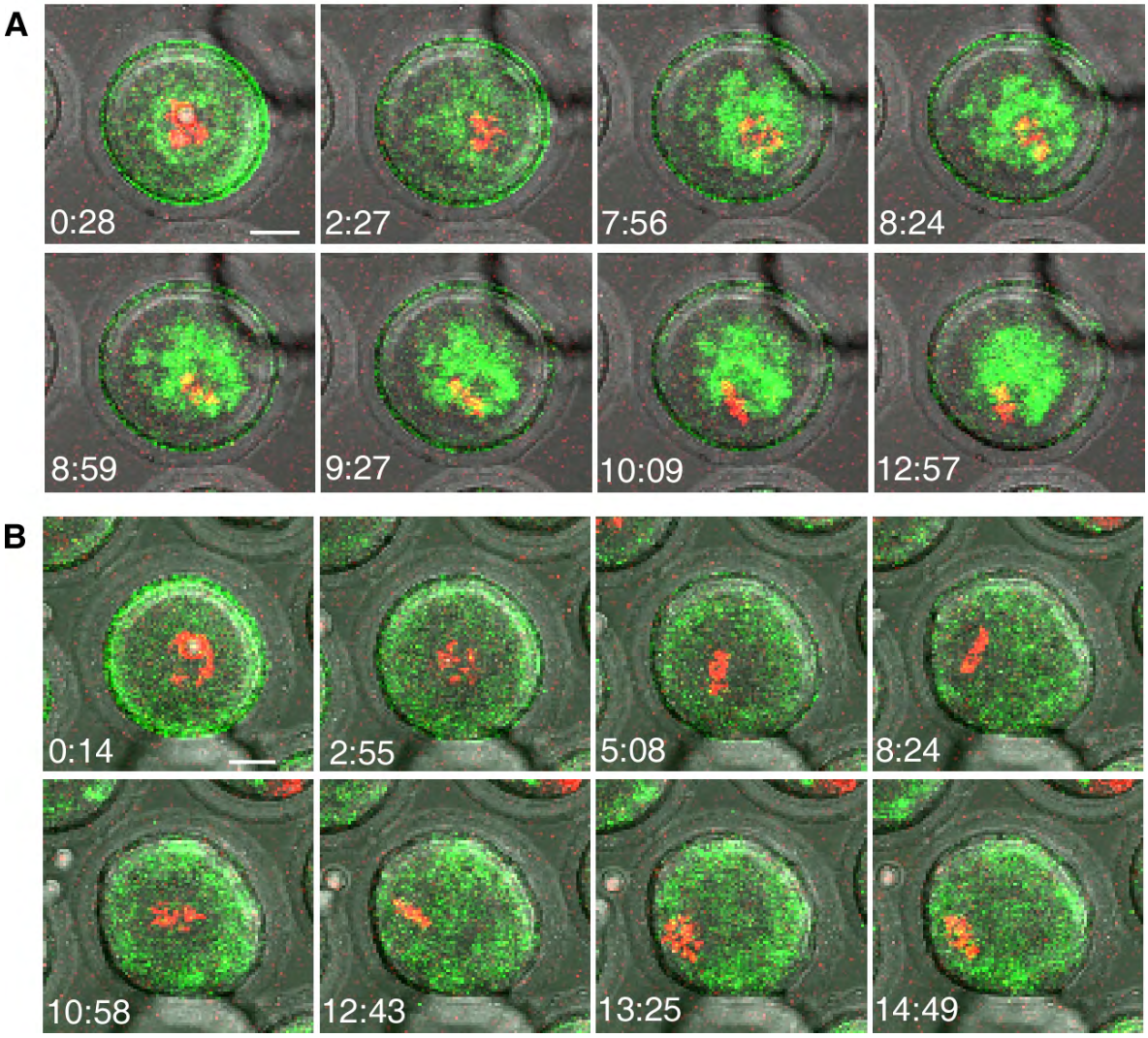

Fig. S6. *Mater*$^{-/-}$ oocytes (B) displayed abnormal EGFP-Fmn2 in cytoplasm during *in vitro* maturation when compared to the wild-type control (A). DNA (red) was labeled by Hoechst 33258. Images were taken from time lapse confocal microscopy at indicated scan time points (hr:min). Scale bars, 20 μm.

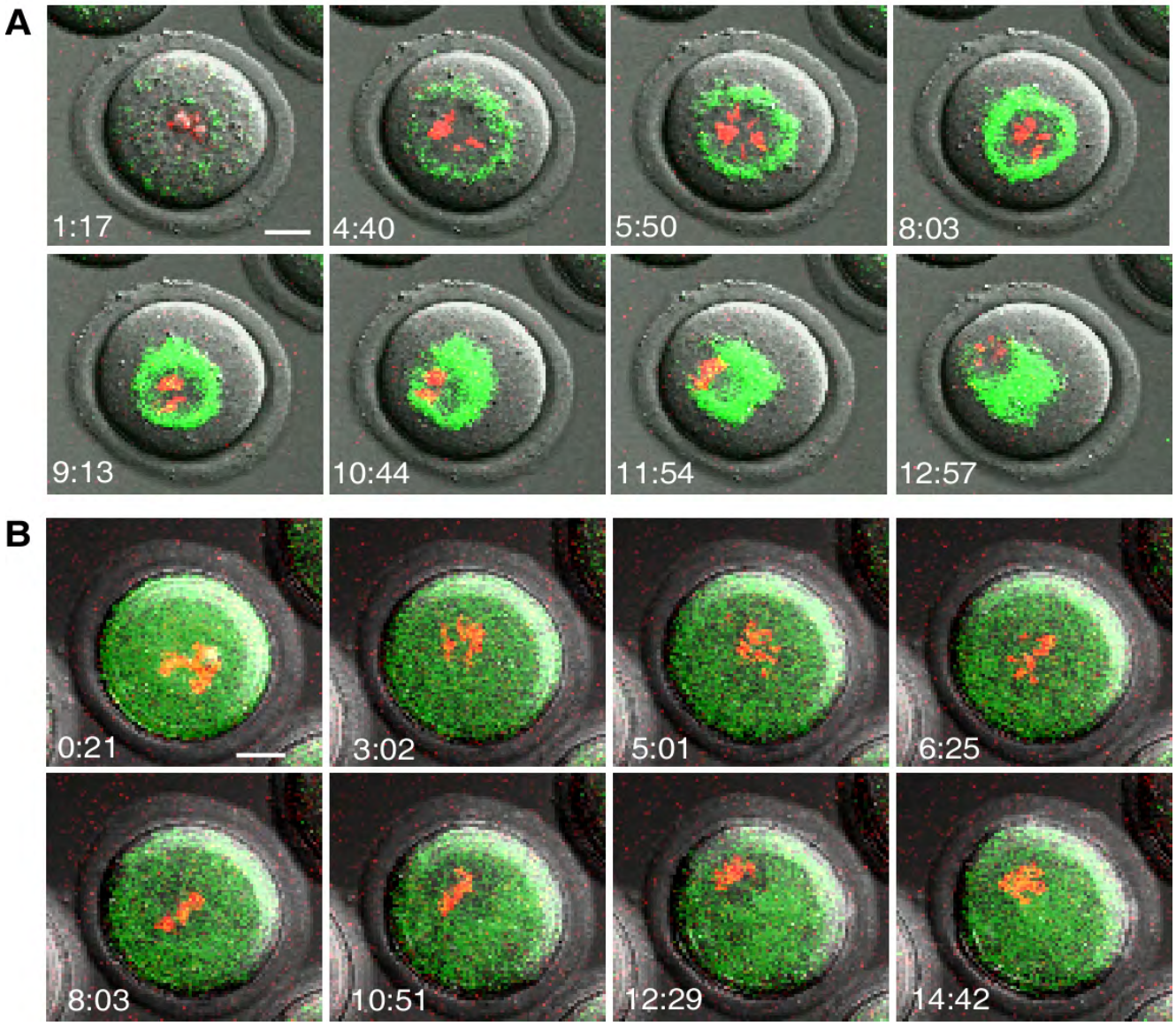

Fig. S7. *Mater*$^{-/-}$ oocytes (B) displayed abnormal Cdc42-GTP in cytoplasm during *in vitro* maturation when compared to the wild-type oocytes (A). Cdc42-GTP was monitored by WASP-CBD-GFP and DNA (red) was labeled by Hoechst 33258. Images were taken from time-lapse confocal microscopy at indicated scan time points (hr:min). Scale bars, 20 μm.

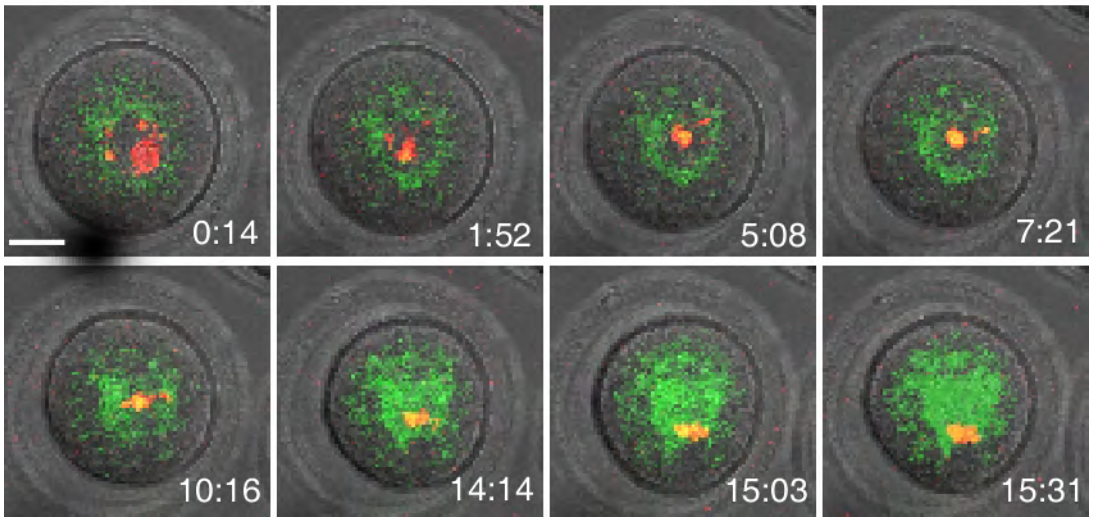

Fig. S8. Dynamic F-actin assembly during meiotic maturation of oocytes from wild-type littermates of *Mater*$^{-/-}$ mice. F-actin was detected with EGFP-LifeAct. DNA (red) was labeled by Hoechst 33258. Images were taken from time-lapse confocal microscopy at indicated scan time points (hr:min). Scale bars, 20 μm.

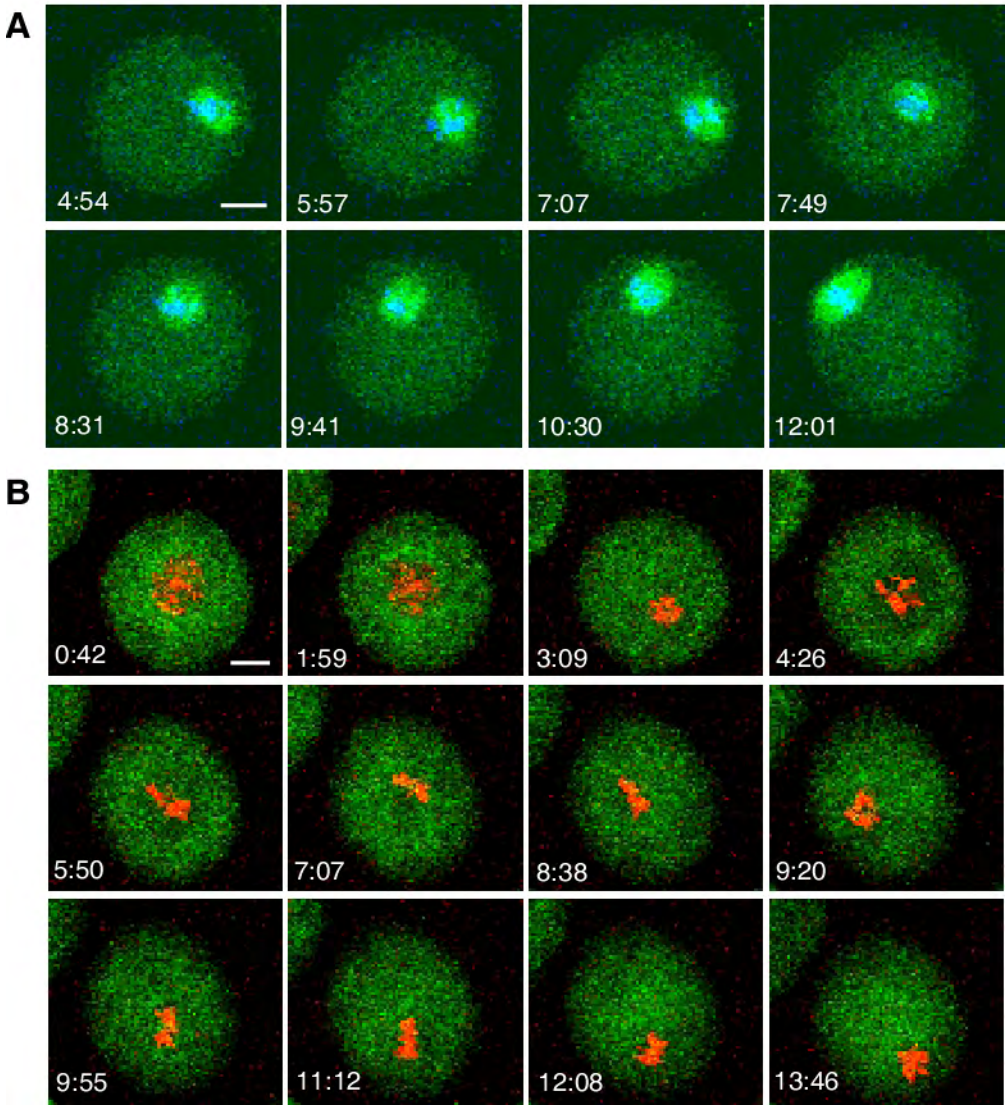

Fig. S9. Oocytes of *Filia*$^{-/-}$ mice (C57BL6×SV129) displayed abnormal spindle movement (A) and PtdIns(3,4,5)P_3 synthesis (B) during in *vitro* maturation. Spindles were visualized with EB1-GFP and PtdIns(3,4,5)P_3 was monitored by PH-Akt-GFP. DNA (blue or red) was labeled by Hoechst 33258. Images in panels A and B were taken from time-lapse confocal microscopy at indicated scan time points(hr:min). Scale bars, 20 μm.

Movie 1. The dynamics of PtdIns(3,4,5)P_3 synthesis monitored with PH-Akt-GFP in normal mouse oocytes during *in vitro* maturation.

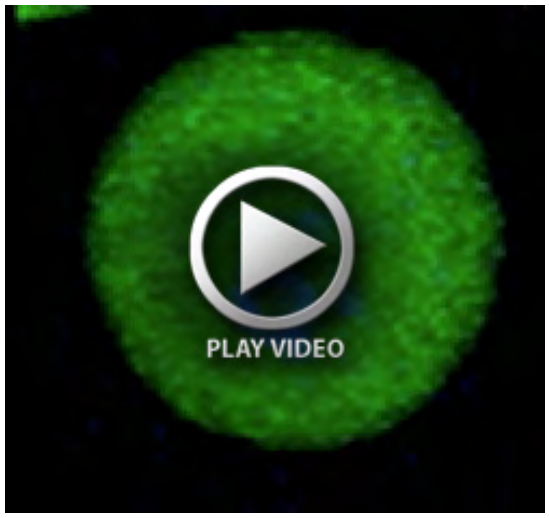

Movie 2. Spindle translocation monitored with GFP-EB1 in normal mouse oocytes during *in vitro* maturation.

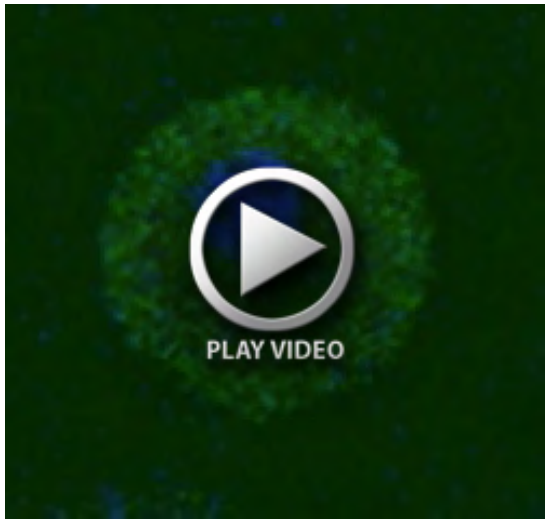

Movie 3. Erratic spindle movement in mouse oocytes treated with LY294002 (20 μM) monitored with GFP-EB1 during *in vitro* maturation.

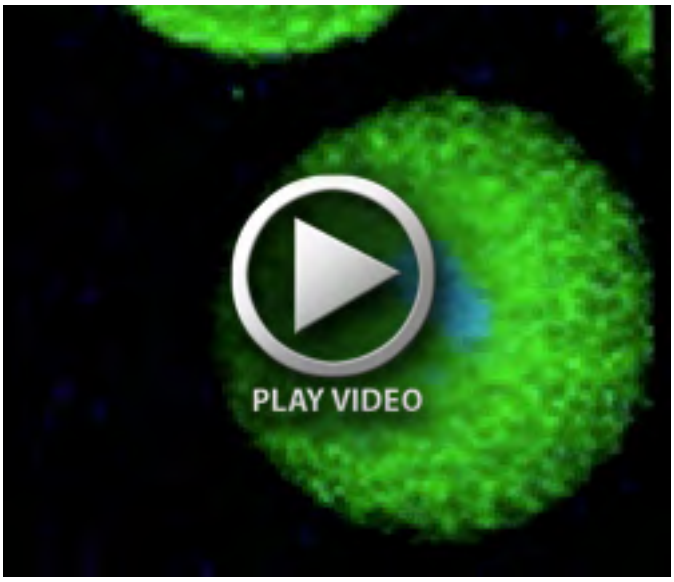

Movie 4. Cdc42 activation in normal mouse oocytes monitored with WASP-CBD-GFP during *in vitro* maturation.

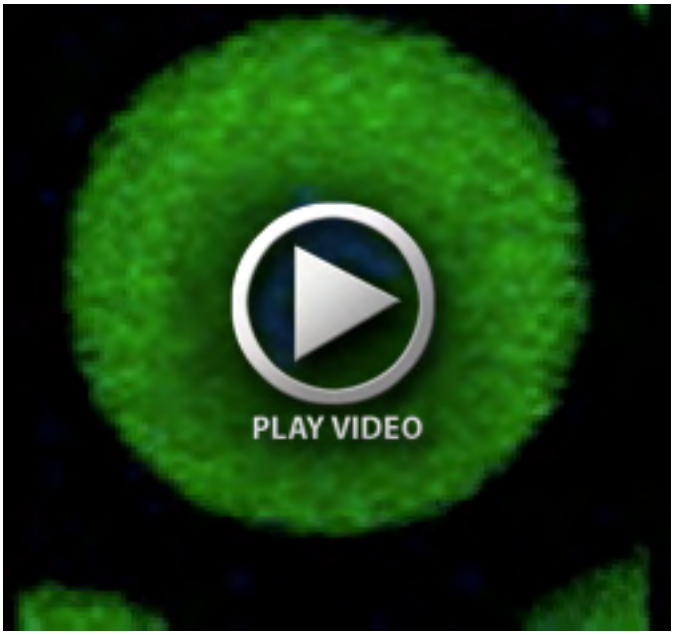

Movie 5. Abnormal spindle translocation in oocytes from *Mater*$^{-/-}$ mice monitored with GFP-EB1 during *in vitro* maturation.